PROGRESS UPDATE
BIOINSPIRED ANTI-ADHESIVE SURFACES

S. Mulansky, M. Saballus and E. Boschke

Technische Universität Dresden, Institute of Natural Materials Technology, Bergstraße 120, 01069 Dresden; Germany
E-mail: elke.boschke@tu-dresden.de

ABSTRACT

Fouling-resistant surfaces, including those that are able to inhibit the growth of biofilms, attracting increasing attention. Our strategy rests upon taking inspiration from nature, in cases where anti-fouling strategies are critical for survival of the given animal or plant.

One of these natural strategies is to suppress the initial adhesion of the biofilm-forming bacteria so that biofilm formation is hindered. For example, the nanotopography of biofilm resistant cicada wings can be mimicked by electrochemical etching of aluminum oxide surfaces. In our work, we examine the anti-adhesion properties of such man-made, bio-similar surfaces.

In this paper, we present our investigation of *Escherichia coli* grown in dynamic culture in a flow through chamber, as well as data from nanoscale measurements of their attachment to these surfaces.

Our experiments showed that the area covered by the biofilm on the nanopatterned surfaces after 16.5 hr of bacterial cultivation was significantly smaller than on planar surfaces. Surprisingly, however, measurements of adhesion strength revealed that bacteria brought into contact with a substrate with a defined force adhered more tightly to the nanopatterned surface. This result can be interpreted in multiple ways, but suggests that other properties in addition to the nanotopography of the surface are important. Therefore, the implementation of nanopatterned surfaces for use in technical equipment, where the inhibition of (bio)fouling is of critical importance, will require testing combinations of particular nanostructures with amphiphilic coatings, a project which is currently underway.

INTRODUCTION

At the Heat Exchanger Fouling and Cleaning XI conference in 2015, we presented our experimental paradigm of biosimilar anti-adhesive surfaces, the design of which are inspired by natural cicada wings. Initial observations of cicada-like chemically etched aluminum oxide-coated surfaces showed reduced bacterial adhesion compared to non-patterned surfaces (Mulansky, et al., 2017).

Current experimental goals are: (i) improving the structure of anti-adhesive surfaces by refined etching methods, (ii) testing of biological cicada wings in a flow chamber developed in-house, (iii) characterization of cell viability of bacteria attached to structured surfaces, (iv) testing the behavior of bacteria other than *E. coli* on nanopatterned surfaces, (v) elucidation of anti-bio-fouling mechanisms in order to facilitate their implementation in technical applications.

In a new project we intend to improve bioinspired, nanopatterned surfaces by increasing the homogeneity of nanopatterns, and by testing the possible inhibitory effects of hydrophobic and hydrophilic coatings on (bio)fouling and thus their potential applications in biofilm-inhibiting surfaces such as heat exchangers.

To achieve this, we have expanded our spectrum of chosen methods from investigations in a flow chamber (Wagner, et al., 2013) on the microscale, to the nanoscale regime. Using an atomic force microscope (AFM) based single-cell force spectroscopy (SCFS) technique, we were able to bring a bacterial cell in contact with an experimental surface, applying a defined loading force (F_l) and contact time (t_c). The detachment force (F_d) then measured is equal to the adhesion force (F_a), The adhesion force and the rupture length (L_r) are both of interest for determining the sticking properties of bacteria which will influence their propensity to form biofilms on a given surface.

MATERIALS AND METHODS

Studying Biofilms, experimental setup

Strains, media, and growth conditions. We used a green fluorescent protein (GFP)-tagged K12 strain of *Escherichia coli* SM2029 (Reisner, et al., 2003) contains pili which enable it to attach to other cells and surfaces.

ISBN: 978-0-9984188-0-3; Published online www.heatexchanger-fouling.com

Surfaces were inoculated with $1 \cdot 10^8/mL$ *E. coli* SM 2029 for at least 30 min and cultivated for 16.5 hr at 30 °C under continuous flow (described in (Mulansky, et al., 2017).

Microscopic analysis of biofilm formation. GFP-tagged bacteria were visualized with an Axioplan 2 imaging (Carl Zeiss Microscopy GmbH, Germany, Zeiss set 38). Live/dead assays were done with propidium iodide (2 mg/L) and examined with a LSM 780/FLIM (Carl Zeiss Microscopy GmbH, Germany, Zeiss sets 38 and 43).

At least 15 images per row were taken from inlet to outlet of the flow chamber in three parallel rows. We used Fiji (ImageJ, Particle Analysis) to calculate the biofilm-covered surface area (%).

Single-cell force spectroscopy measurements. Bacteria were loaded on aminated polyethyleneimine (PEI) coated silica beads (PSI-20.0NH2 (Kisker Biotech GmbH, Germany)). *E. coli*-PEI-bead complexes were attached on a V-shaped tipless cantilever (PNP-TR-TL-Au (200 µm), NanoWorld AG, Switzerland) using UHU Plus Schnellfest (UHU GmbH & Co. KG; Germany).

To evaluate bacteria prior to or during SCFS measurements *E. coli*-PEI-bead complexes were positioned under an Axio Observer D.1 fluorescence microscope (Carl Zeiss Microscopy GmbH, Germany, Zeiss set 8) housed in the NanoWizard® II AFM (JKP Instruments).
The cantilever with the attached *E. coli*-PEI-bead was transferred to the substrate with an approach and retraction speed of 10 µm/s. Force-distance curves were recorded using a loading force (F_l) of 10 nN and a contact time (t_c) of 10 s, on at least 3 randomly chosen areas, each with 3 x 3 measurement points 33.3 µm apart.

Surfaces. Porous anodized aluminum oxide membranes (Al_2O_3) with well-defined surface nanopatterns were fabricated as stated earlier (Mulansky, et al., 2017). The solid-surface fractional area was calculated by analyzing scanning electron micrographs of the nanopatterned surfaces using Fiji.

RESULTS

Our main goal was to learn about structural and functional mechanisms that cicada wings have evolved that enable these insects to resist bacterial deposition and growth, i.e. biofilm formation. In order to achieve this, we tested adhesion behavior of *E. coli* bacteria on artificial nanopatterned surface inspired by cicada wings in our system under continuous flow of minimal medium (for the method, see (Mulansky, et al., 2017) .

Scanning electron microscope (SEM)- und atomic force microscope (AFM)-images of planar and nanopatterned experimental surfaces produced by electrochemical etching that were tested for bacterial adhesion and growth are shown in **Error! Reference source not found.**.

The nanopatterned surfaces are made starting with a planar surface that has a corrugated structure with a peak to peak distance of > 10 µm, and a height of several micrometres. The nanopattern is created in this surface via a two-step anodization process (Mulansky, et al., 2017), whereby pores are first etched with a diameter of 300 nm, and in a second step widened to form needle-like structures.

As can be seen in **Error! Reference source not found.** (below right), AFM measurements were unable to detect the true depth profile of the pores, which according to the manufacturer of the nanopatterned surfaces (SmartMembranes GmbH) should be < 60 µm.

ISBN: 978-0-9984188-0-3; Published online www.heatexchanger-fouling.com

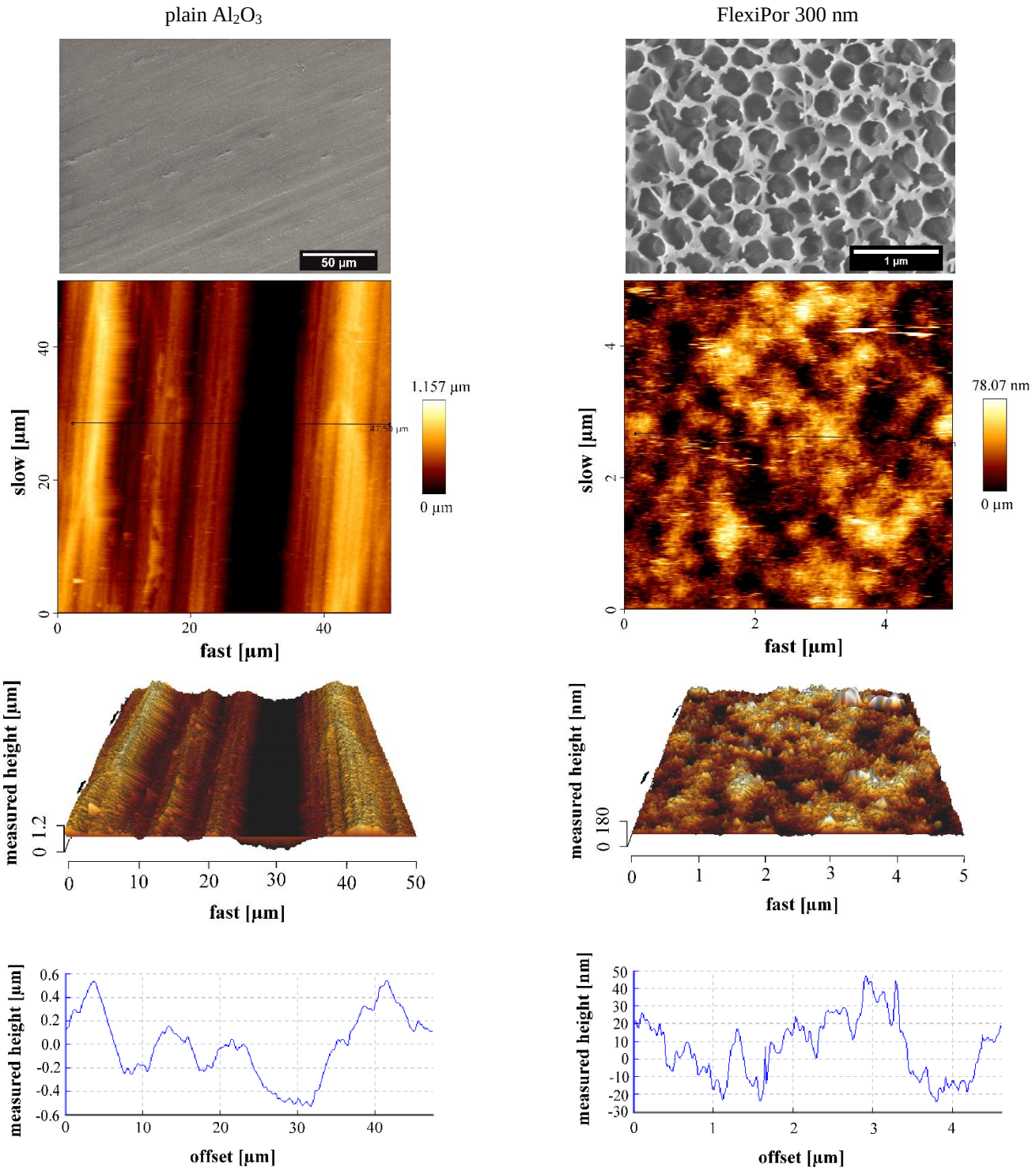

Figure 1 SEM and AFM-images taken from plain and etched Al_2O_3 (FlexiPor 300 nm). From top to bottom: SEM; AFM top-view and AFM 3D images; height profiles of the AFM scans

Live/dead assays with propidium iodide were carried out in order to judge the extent of coverage of the surfaces with biofilm, and the percentage of living bacteria in biofilms grown on planar and nanopatterned surfaces for 16.5 hr in the flow chamber (Figure 2).

3D images of *E. coli*-PEI-beads after staining with propidium iodide show that only a small proportion of the bacteria were stained in red, while the majority of bacteria (showing green fluorescence) remained alive (Figure 3). In our experiments, one PEI-Bead coated with an *E. coli* monolayer, similar to the one shown in Figure 3, was affixed to the cantilever for subsequent SCFS measurements in order to quantify the degree of microbial adhesion, as an initial requisite step for biofilm initiation. The implementation of this approach enabled us to gain an understanding into the nanoscale mechanics of early-stage bacterial adhesion and thus biofilm formation.

ISBN: 978-0-9984188-0-3; Published online www.heatexchanger-fouling.com

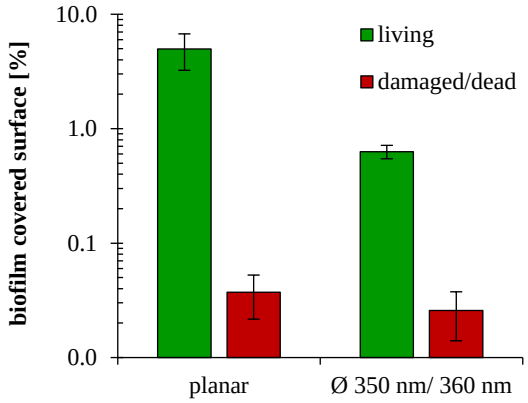

Figure 2 Comparison of the surface area covered by biofilm [%] on planar vs. nanopatterned aluminum oxide surfaces.

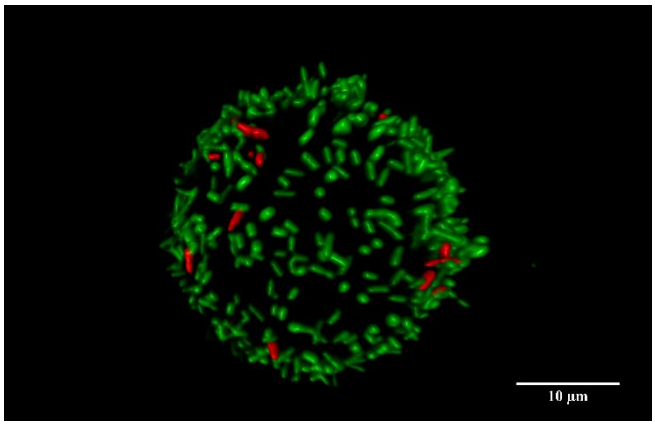

Figure 3 3D Fluorescence image of a PEI-Bead coated with *E. coli*.

Selected SCFS measurements are shown in Figure 4 as histograms of relative frequencies (%) of F_d and L_r data obtained in the given range bins on reference vs. nanostructured surfaces.

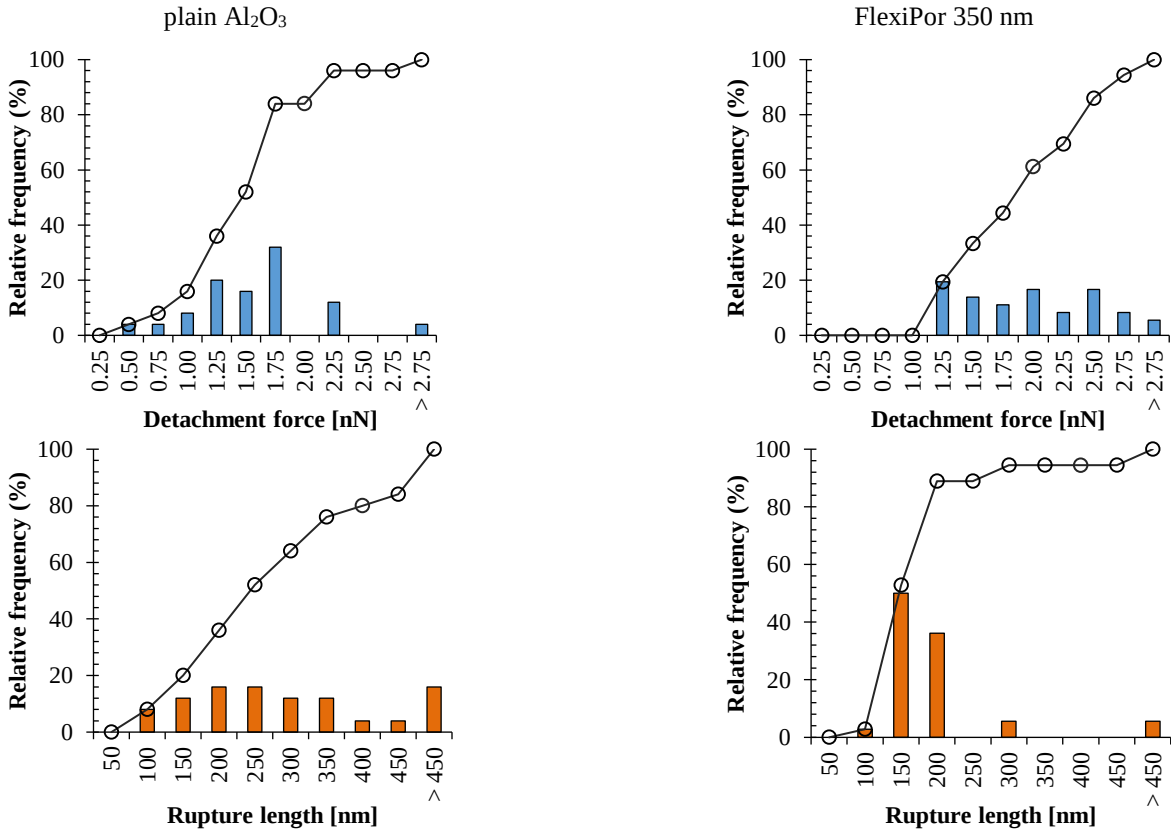

Figure 4 Relative frequency (%) of detachment force (F_d) and rupture length (L_r) on planar (A, C; n = 25) and nanopatterned (B, D; n = 36) surfaces. Black lines indicate sum functions.

DISCUSSION

Nanopatterned surfaces may be anti-fouling because they're either anti-microbial, or they inhibit adhesion of the bacteria. The live/dead staining result indicates that they're not anti-microbial per se. Live/dead-staining of bacteria grown on artificially nanopatterned vs. unstructured surfaces showed no differences in viability (1 % vs. 4 % (Figure 2)), indicating that the nanopatterned surfaces lack antimicrobial properties, and suggesting rather that reduced biofilm growth is due to prevention of bacterial adhesion. Thus, the ability of bacteria to adhere to a surface appears to be an important

determining factor in the propensity of the surface to resist biofilm formation. Two factors, namely elasticity and the presence of biomolecules on the bacterial outer membrane, are important determinants of bacterial adhesion.

In wild *E. coli* strains, LPS constituting ~75 % of the outer cell membrane participate in primary adhesion, as is the case with all gram negative bacteria (Lu, et al., 2011). The strain used here, *E. coli* SM 2029, is a so-called K 12 strain, and lacks the O-antigen portion in LPS. As a result, the monosaccharides of the core region, which carry phosphate and carboxylic groups form a net negative charge at the outer surface of the bacterium. It can participate in non-specific electrostatic interactions with hydrophilic surfaces, such as that presented by aluminum oxide. We propose that the majority of the observed interactions reflected in the F_d values measured on both smooth and nanopatterned surfaces, and thus the equivalent adhesion forces F_a, could be accounted for by these electrostatic interactions.

The peritrichous flagellated *E. coli* strain SM 2029 is known to be proficient in biofilm formation. This is thought to be due to its extensive formation of pili that are in the range of 0,1 - 1 µm in length, and ~2 - 8 nm in diameter (Reisner, et al., 2003). The adhesion of bacteria to surfaces has been ascribed predominantly to the presence of these pili, and the pilin protein found therein, as well as to flagellin present in flagellar structures also found on their surfaces (Miller, et al., 2006). We propose that in the case of *E. coli* SM 2029, which lacks O-Antigen region and therefore has only a core region of LPS with 4 nm in thickness, adhesion is achieved through proteins present on the cell surface.

As can be seen in Figure 4, the F_ds of *E. coli*-PEI-beads brought into contact with the nanopatterned surfaces were larger than those seen on the unstructured surfaces. This appears to contradict the finding that biofilm formation measured in Figure 2 was less robust on the nanopatterned surfaces than on the smooth surfaces, which would initially suggest that the bacteria more readily adhere to the smooth surface (reference surface). While we cannot rule out that such apparent contradictions in our findings arise from differences in experimental particulars of the two methods we applied: in the case of SCFS measurements, bacteria are pressed onto a surface with a force F_l of 10 nN, whereas in the flow-through chamber where biofilm formation was assayed, the bacteria were allowed to sediment in the chamber for 30 min before the flow of media began. However, the SCFS measurements allow certain conclusions to be drawn about adhesion mechanisms.

With a view to the aforementioned factors that might have influenced the outcome of the SCFS experiments, the following interpretation of the results can be made: in the case of the unstructured reference surface, it is possible that protein chains of pilin and flagellin might be forced or folded together upon contact with the planar surface. If this were the case, dissociation would be expected to occur stepwise, leading to a wide distribution of values for L_r (as is seen in Figure 4, bottom left). The measured values of F_d are also consistent with this interpretation. In this scenario, the tangled protein chains would break free individually from the substrate surface through a reduction of the contact surface. During contact with the nanopatterned surfaces, the hair-like appendages (pili and flagella) would potentially encounter a larger surface to which adhesion is possible on the side-walls of the pores, without being compressed before contact. It should be pointed out that according to the manufacturers of the nanopatterned surfaces that were used in this study, the pores are several µm deep, whereby the pore depth shown in **Error! Reference source not found.** (bottom right) is not accurately reflective of the actual depth, due to a limited depth range of the cantilever.

Consistent with a depth matching the manufacturer's specifications our findings, that on the nanopatterned surfaces the measured F_d was always larger than 1.25 nN (see Figure 4 top right), and the L_r values were mainly between 150-200 nm (Figure 4, bottom right), can be explained.

An additional consideration is that the unexpectedly high values for F_d on the nanopatterned surface, given their apparent resistance to biofilm formation, are likely related to the elasticity - given by Young's modulus E - of the relatively thin (several nm) gram-negative cell wall of the *E. coli* strain used in this study.

Further on the elastic properties of these particular cell walls, an E of 0.365 ± 0.122 MPa was measured for *E. coli* in PBS by Chen (Chen, et al., 2009). Measurements in pure distilled water, in contrast, gave values of 12.8 ± 0.1 MPa (Abu-Lail and Camesano, 2006). These higher values of E in the water can be explained by the effect on cell membrane stiffness because of water entering the cell through osmotic pressure. The influence of LPS on cell elasticity was also shown by Chen and colleagues, (Chen, et al., 2009) who found that removal of LPS by ethylenediaminetetraacetic acid (EDTA) significantly lowered E (0.101 ± 0.056 MPa). It should be noted, indeed, that EDTA does not remove the LPS but as a divalent metal cation-chelating agent breaks the divalent cation-mediated salt bridges between lipopolysaccharides (Li, et al., 2016).

Other authors found E values up to 221.4 ± 1.9 MPa in *E. coli*, depending on the strain and measurement conditions, albeit these were non-physiological (Eaton, et al., 2008) (Table 1).

Through these earlier studies and by using the Hertz model (Dintwa, et al., 2008), we were able to estimate the deformation δ (Chen, et al., 2012). In this model, bacteria are approximated as uniform elastic spheres that can be pressed onto a smooth surface with a normal force F. The deformation is then calculated according to the following formula (1):

$$\delta = \left(\frac{9 \cdot F^2}{16 \cdot R \cdot E^{*2}}\right)^{\frac{1}{3}} \quad (1)$$

In our case, the applied normal force F is equivalent to the loading force F_l (10 nN), and R is the radius of the cell. E^* is commonly referred to as the effective stiffness, and reflects the elastic properties of the cell (2):

$$E^* = \frac{E}{1-\nu^2} \quad (2)$$

with the Poisson's ratio ν. For soft biological material such as bacteria, the value of ν is assumed to be 0.5 (Touhami, et al., 2003).

Since our AFM measurements are carried out in PBS (phosphate-buffered saline), and the *E. coli* strain used lacks O-Antigen region, we can assume an E^* between 0.49 and 0.13 MPa (as measured according to (Chen, et al., 2009)). Thus for a cell with a radius of 0.25 µm and an applied loading force F_l of 10 nN, the cell would theoretically undergo deformation up to 200 nm in the direction in which the force is applied. As a consequence of this elastic deformation, the contacting surface of the cell wall to the substrate would be enlarged.

To what extent these considerations may be applicable to the interactions of bacteria with nanopatterned surfaces, is still unclear. However, one can speculate that the combined effects of bacterial deformation together with the adherent properties of the pili and flagella explain the surprisingly high values we obtained for F_d, through a possible increase in interaction surface between the bacterial wall and the nanopatterned surface.

Table 1 Young´s modulus (E) measured in *E. coli* under different conditions yields the effective stiffness E^* and the deformation δ of the cell with a radius R = 0.25 µm subjected to an applied loading force of F_l = 10 nN, estimated on smooth surface.

E (MPa)	E^* (MPa)	δ (nm)	Organism Method of measurement of Young's Modulus	Source
0.365 ± 0.122	0.49	98.3	native bacteria with LPS, in PBS	(Chen, et al., 2009)
0.101 ± 0.056	0.13	231.5	native bacteria (pretreated with EDTA), in PBS	(Chen, et al., 2009)
12.8 ± 0.1	17.07	9.2	native bacteria in distilled water	(Abu-Lail and Camesano, 2006)
221.4 ± 11.9	295.20	1.4	dehydrated bacteria in air	(Eaton, et al., 2008)

CONCLUSIONS AND OUTLOOK

Our measurements of bacterial adhesion on nano-patterned surfaces demonstrated that although these surfaces have an anti-biofilm effect, cells may adhere more tightly to structured surfaces than to smooth ones. Analyses carried out in the nanoscale via AFM revealed that the cells are in fact more adherent to the nanopatterned surface when applied with a loading force of 10 nN, contrary to our assumptions from findings in microscale of their reduced ability to form biofilms on these surfaces

Many questions remain unanswered, including that concerning the molecular mechanism of adhesion, or the density of adhesion points that are required on the surface for a biofilm to form. We were, however, able to prove that the nanopatterned materials we used were not anti-adhesive per se, but neither were they antimicrobial, since the viability of the adhering bacteria was unaffected.

Further investigation will be required to clarify these issues and will involve, among others, the investigation of the effects of chemically etched surfaces and coating with a novel amphiphilic anti-adhesive that may also have biocidal properties. Concrete plans include the testing of real-world fouling conditions such as those found in heat-exchangers - currently in focus are those used in saltwater desalination plants. Our contributions will entail the microscopic examinations of (bio)fouling. These will be carried out in the flow chamber (described here (Mulansky, et al., 2017)), equipped with new microfluidics, as well as in a flow tube designed after a Robbins-Device with multiple removable sample holder (see Fig. 5).

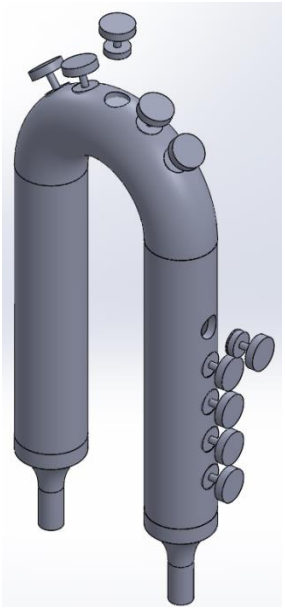

Figure 5 Theoretical design of a flow cell with multiple removable sample holder

ACKNOWLEDGEMENT

We acknowledge the valuable help in CLSM (confocal laser scanning microscopy) provided by Dr. Ruth Hans and Dr. Hella Hartmann of the Light Microscopy Facility at the Biotechnology Center of the TU Dresden. We would also like to thank Dr. Jens Friedrichs of the Max Bergmann Center at TU Dresden for giving us the opportunity to carry out the SCFS measurements. This work was supported by the Central Innovation Program SME (Zentrales Innovations-programm Mittelstand [ZIM]) of the Federal Ministry for Economic Affairs and Energy, Germany (KF2049818).

NOMENCLATURE

AFM	atomic force microscope
Al_2O_3	porous anodized aluminum oxide
CLSM	confocal laser scanning microscopy
E	Young´s modulus, MPa
E^*	effective stiffness, MPa
EDTA	Ethylenediaminetetraacetic acid
F	force, nN
GFP	green fluorescence protein
L	length, nm
LPS	lipopo
PBS	phosphate-buffered saline
PEI	polyethylenimine
R	radius, µm
SCFS	single-cell force spectroscopy
SEM	scanning electron microscopy
t	time, s
δ	deformation, nm
ν	Poisson's ratio, dimensionless

Subscript

l	loading
d	deformation
a	adhesion
r	rupture
c	contact

REFERENCES

Abu-Lail Nehal I. and Camesano Terri A., 2006, The effect of solvent polarity on the molecular surface properties and adhesion of Escherichia coli, *Colloids and Surfaces B: Biointerfaces*, Vol. 51, pp. 62-70.

Chen Yi-Yang, Wu Chien-Chen, Hsu Jye-Lin, Peng Hwei-Ling, Chang Hwan-You and Yew Tri-Rung, 2009, Surface Rigidity Change of Escherichia coli after Filamentous Bacteriophage Infection, *Langmuir*, Vol. 25, pp. 4607-4614.

Dintwa E., Tijskens E. and Ramon H., 2008, On the accuracy of the Hertz model to describe the normal contact of soft elastic spheres, *Granular Matter*, Vol. 10, pp. 209-221.

Eaton Peter, Fernandes João C., Pereira Eulália, Pintado Manuela E. and Xavier Malcata F., 2008, Atomic force microscopy study of the antibacterial effects of chitosans on Escherichia coli and Staphylococcus aureus, *Ultramicroscopy*, Vol. 108, pp. 1128-1134.

Li M., Gan C. Y., Shao W. X., Yu C., Wang X. G. and Chen Y., 2016, Effects of membrane lipid composition and antibacterial drugs on the rigidity of Escherichia coli: Different contributions of various bacterial substructures, *Scanning*, Vol. 38, pp. 70-79.

Lu Q. Y., Wang J., Faghihnejad A., Zeng H. B. and Liu Y., 2011, Understanding the molecular interactions of lipopolysaccharides during E. coli initial adhesion with a surface forces apparatus, *Soft Matter*, Vol. 7, pp. 9366-9379.

Miller E., Garcia T., Hultgren S. and Oberhauser A. F., 2006, The mechanical properties of E-coli type 1 pili measured by atomic force microscopy techniques, *Biophys. J.*, Vol. 91, pp. 3848-3856.

Mulansky Susan, Goering Petra, Ruhnow Maria, Lenk Felix, Bley Thomas and Boschke Elke, 2017, A Modular Flow Cell System for Studying Biomimetic and BioinspiredAnti-Adhesive and Antimicrobial Surfaces, *Heat Transfer Engineering*, Vol. 38, pp. 805-817.

Reisner A., Haagensen J. A. J., Schembri M. A., Zechner E. L. and Molin S., 2003, Development and maturation of Escherichia coli K-12 biofilms, *Mol. Microbiol.*, Vol. 48, pp. 933-946.

Touhami Ahmed, Nysten Bernard and Dufrêne Yves F., 2003, Nanoscale Mapping of the Elasticity of Microbial Cells by Atomic Force Microscopy, *Langmuir*, Vol. 19, pp. 4539-4543.

Wagner Katrin, Friedrich Sandra, Stang Carolin, Bley Thomas, Schilling Niels, Bieda Matthias, Lasagni Andrés and Boschke Elke, 2013, Initial phases of microbial biofilm formation on opaque, innovative anti-adhesive surfaces using a modular microfluidic system, *Eng. Life Sci.*, Vol. 14, pp. 76-84.